

**PAPER TYPE (Research paper)**

## Implementation of human body tissues model in FPGA

**Hossein Salarabedi<sup>1</sup>, Seyyed Javad Seyyed Mahdavi<sup>2</sup>, Mohammad Javadian Sarraf<sup>3</sup>, Hamidreza Kobravi<sup>4</sup>**<sup>1</sup>Department of Electrical Engineering, Mashhad Branch, Islamic Azad University, Mashhad, Iran<sup>2</sup>Department of Electrical Engineering, Mashhad Branch, Islamic Azad University, Mashhad, Iran<sup>3</sup>Department of Electrical Engineering, Mashhad Branch, Islamic Azad University, Mashhad, Iran<sup>4</sup>Research Core of Robotic Rehabilitation and Biofeedback, Mashhad Branch, Islamic Azad University, Mashhad, Iran

---

**Article Info****Article History:**

Received: 9 August, 2024

Revised: 20 September, 2024

Accepted: 1 October, 2024

**Keyword:**FPGA, Electrical modeling,  
Zing hardware

Corresponding

Author's

Email Address:

javad.mahdavi@gmail.com

---

**Abstract**

The electrical modeling of the human body in the form of electrical elements such as resistors and capacitors has simplified the analysis of the body for researchers and doctors. There are various models for the body. One of the most famous of these models is the Cole model, which is used for the inside and outside of body cells. This model is a combination of several resistors and capacitors that are made and modeled in different ways. In some researches, it is made as a real resistor and capacitor, and in others, it is simulated in electrical circuit analysis software. In this research, the body model has been implemented in FPGA, which is used to analyze body tissues, including bioimpedance measurement, and its inputs and outputs have been recorded. Finally, the program is implemented in Zing hardware and its inputs and outputs are displayed by a digital oscilloscope. In FPGA compared to previous works, from the perspective of hardware volume and accuracy has been improved.

**Introduction:**

The implementation of The study of the electrical properties of body tissues is an important area of research. Due to the sensitivity of tests performed on real body tissues, researchers are increasingly interested in using electrical models of the body. Research on the electrical properties of body tissues dates back to the 18th century. In 1928, Cole proposed a description of zero and infinite frequencies[1]. He also introduced the concept of the Constant Phase Element (CPE) and was the first to depict the eminence (a term used in place of impedance and admittance) on the Wessel diagram, now known as the Cole diagram. Additionally, he developed a three-element model consisting of two resistors and a capacitor to represent the body[2].

Research in this field has primarily been conducted using three main platforms. The first platform involves constructing an electrical model using physical elements such as resistors and capacitors. This approach offers simplicity and availability but has the drawback of lower accuracy. For example, reference [3] discusses the use of highly precise resistors and capacitors

with tolerances up to 0.01%. Some research has employed switched capacitors in RC circuits, which are in series with a resistance and then paralleled with another resistance [4]. The body model has been physically implemented, with impedance measurements accounting for the resistances and capacitances of both the electrode and the connection point to the tissue, all within a package known as the body simulator module [5]. Other researchers have designed and constructed the body model directly on a board [6][7]. Ahmed Al-Hashimi and colleagues have used Bio-Z, which features a capacitive resistance package for each tissue type, including a connection point for electrodes for current delivery or voltage measurement, making it highly suitable for measuring tissue bioimpedance [8]. Saul Rodriguez and his team introduced a model where the entire tissue model and electrodes are integrated into one package. This package uses gold-plated electrodes and is made from Rogers 4000 hydrocarbon ceramic. The body model is a grid with two openings and four heads, constructed from semiconductor layers with dimensions of 3 mm, incorporating different permittivity and conductivity values for various tissues. While this design offers

Doi:

H. Salarabedi *et al.*

high precision and small dimensions, it is more complex and costly to manufacture. The lowest impedance value recorded is 107 ohms for blood tissue, while the highest is 2491 ohms for bone skeleton tissue [9].

The second platform involves simulation programs such as SPICE and MATLAB, where the electrical model of the body is simulated. This approach increases accuracy, but it cannot be implemented physically. For instance, LTspiceIV from Linear Technology has been used in some studies to simulate the body model with high accuracy; for example, values such as  $S = 19.9 \Omega$ ,  $R_P = 19.86 \Omega$  and  $C_P = 99.7$  can be obtained [6]. Bassem Ibrahim and colleagues have accurately implemented the body model using MATLAB software and measured its bioimpedance [10]. The third platform involves implementation in systems on a chip, such as FPGA, which offers both high accuracy and the possibility of physical implementation. Research in this area is less extensive, presenting significant opportunities for further study and implementation of body models. One notable approach in this field involves the use of Look-Up Tables (LUTs). In this method, impedance and phase are measured using relationships between the size sections, with the phase difference achieved through delay and amplitude adjustments via multipliers. The delay and amplitude change values for each part or body tissue are stored and implemented in the FPGA [11].

In the proposed method of this research, phase and amplitude values are calculated independently for each tissue, and the real model of different body tissues is implemented in FPGA. First, the body tissue model is examined. Then, the method of implementing the model in FPGA is described, and the results are validated using several body tissue samples.

**Materials and methods:**

Initially, the conventional electrical model of different body tissues is explained. This model is then implemented in FPGA.

**Model body tissues:**

If electric current passes through the body at low frequencies, it primarily flows through the extracellular water (ECW) or extracellular fluid (ECF), while the cell membrane acts as a capacitor. At high frequencies, both the extracellular water (ECW) and intracellular water (ICW) or intracellular fluid (ICF) conduct the current, as illustrated in Fig. 1 [12].

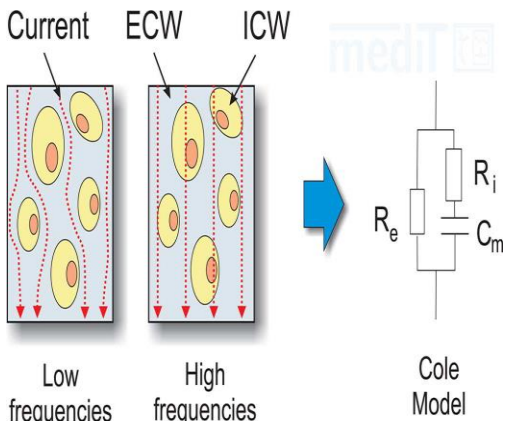


Fig. 1: Current Flow and ECW and ICW

The equivalent circuit of body tissue consists of a resistance  $R_e$  corresponding to the extracellular space, in parallel with a resistance  $R_i$ , which is in series with a capacitor  $C_m$  presenting the cell membrane. This impedance model is known as the Cole model.

$$Z(j\omega) = \frac{u(j\omega)}{i(j\omega)} \tag{1}$$

Using Cole's model, impedance is expressed as Equation 2.

$$Z(j\omega) = \frac{u(j\omega)}{i(j\omega)} = \frac{R_e \cdot (R_i + \frac{1}{j\omega C_m})}{R_e + R_i + \frac{1}{j\omega C_m}} = \left( \frac{R_e}{R_i + R_e} \right) \cdot \left( R_i + \frac{R_e}{1 + j\omega C_m (R_e + R_i)} \right) \tag{2}$$

Real and imaginary parts are in Relation 3:

$$\begin{aligned} Re\{Z\} &= \frac{R_e + \omega^2 C_m^2 R_i R_e (R_i + R_e)}{1 + \omega^2 C_m^2 (R_i + R_e)^2} \\ Im\{Z\} &= \frac{\omega C_m R_e^2}{1 + \omega^2 C_m^2 (R_i + R_e)^2} \end{aligned} \tag{3}$$

At low and high frequencies, the impedance behaves as resistance. Fig. 2 shows the diagram of impedance changes with respect to frequency, illustrating this behavior.

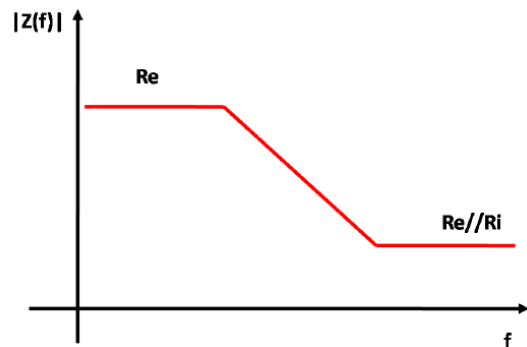


Fig. 2: Impedance Magnitude as a Function of Frequency

**Implementation in FPGA :**

In this section, the body model is implemented inside the FPGA. First, we introduce the inputs and outputs of this section. The inputs include `in_data`, `'clk,R1,R2` (in picofarads), and `cycle_cont'`. The outputs are `out_data` and `z`. Fig. 3 shows the general block diagram of this section.

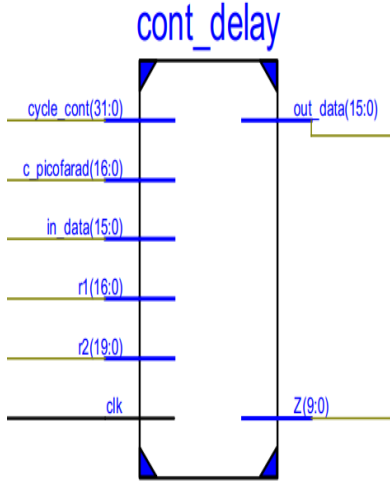


Fig. 3: General Block Diagram of the cont\_delay Section for Implementing the Body Model in FPGA

To understand the function of this section, we review Figure 1 again, with the difference that instead of  $R_e$ , we use  $R_1$ ; instead of  $R_i$ , we use  $R_2$ ; and instead of  $C_m$ , we use  $C$ . The value of the phase  $\theta$  of the impedance is derived using Relations 3 in the form of Relation 4.

$$\theta = \operatorname{tg}^{-1} \frac{2\pi R_1 C f}{1 + 4\pi^2 R_2 C^2 f^2 (R_1 + R_2)} \quad (4)$$

At first, the value of  $\theta$  is obtained according to the inputs. Another point is that the number of clocks in a cycle is known from the cycle\_cont' input, which itself is obtained from the cycle\_counter` block. If we denote the number of clocks in one cycle as  $n$ , then the number of clocks in the phase difference, or in other words the input delay  $m$ , is obtained from Equation 5.

$$m = \frac{2\pi}{n} \times \theta \quad (5)$$

We have 7 clocks with 7 different frequencies and 5 body tissues, including 2 muscle tissues, skin tissue, fat tissue, and bone tissue. The values of  $R_1$ ,  $R_2$ , and  $C$  are provided according to Table 1 for these different body tissues.

Table 1: Values of  $R_1$ ,  $R_2$ , and  $C$  for Different Body Tissues

Texture	R1	R2	c
fat	100	900 kΩ	30 pF
		kΩ	
1 Muscle	1 kΩ	800 Ω	100 nF
Skin	10 kΩ	7.8 kΩ	2. nF
Muscle 2	100 Ω	83 Ω	35 nF
bone	20 kΩ	16.5 kΩ	3 nF

Each of the above tissues is calculated at 7 frequencies and stored in an LUT table. For each value of  $m$ , which represents the number of pulses by which the original sinusoidal signal needs to be delayed in the FIFO loop, the FIFO is implemented in software using the ISE program. In this setup, the input signal is shifted by one cycle to achieve the value of  $m$ . The shifted output is out\_data. This output retains its amplitude but has been adjusted in terms of phase to the required size.

### Simulation Results

First, it is necessary to verify the impedance of each tissue and evaluate how closely the values stored in the LUT in the FPGA match the actual values for each tissue.

### Validation of the results o the body phantom part

As can be seen from Table 1 , the values of  $R_1$ ,  $R_2$ , and  $C$  for the basic body tissues are taken from authoritative sources. Based on these 5 body tissues and their values at 7 different frequencies, an LUT is formed as shown in Table 2 for phase and Table 3 for amplitude. This table is used in phase calculations.

Table 2: Phase LUT Table for Different Tissues and Frequencies

Frequenc y value	adipose tissue	Muscle 1 tissue	bone	Muscle 2 tissue	skin texture
<b>10</b>	2.99819	11.6685	6.16251	17.4772	16.5342
		4		2	2
<b>20</b>	2.57107	6.19880	11.5776	22.8498	9.55404
		8	0	8	
<b>30</b>	1.56584	3.14924	18.7749	19.9376	4.97629
		8	8	8	
<b>40</b>	1.08785	2.10579	21.6613	15.5959	3.34357
			4	1	
<b>50</b>	0.82809	1.58100	22.0174	12.4780	2.51460
			7	8	
<b>60</b>	0.66709	1.26541	21.1893	10.3059	2.01425
			6	4	
<b>70</b>	0.47941	0.90425	18.5052	7.57739	1.44036
			3		

Table 3: Amplitude LUT Table for Different Tissues and Frequencies

Frequency kHz	adipose tissue	Muscle 1 tissue	bone	Muscle 2 tissue	skin texture
10	954.264	4.7102	0.9844	86.552	103.218
	90	51	2	44	06
20	922.892	4.5139	0.9430	69.315	93.9817
	30	3	2	31	8
30	906.912	4.4620	0.8292	53.897	91.3309
	31	2	9	82	6
40	903.195	4.4522	0.7272	48.884	90.8221
	16	7	5	27	9
50	901.822	4.4488	0.6533	46.809	90.6427
	83	5	6	94	4
60	901.174	4.4472	0.6025	45.779	90.5594
	33	6	1	30	4
70	900.602	4.4458	0.5427	44.841	90.4867
	62	8	68	19	7

To validate the implementation of the body phantom in the FPGA, the model is separately implemented in the ISE program, and the entire table above is extracted from this model. The program has a general block diagram as shown in Figure 4, where cycle\_cont represents the total number of clocks in one cycle, 'R1', 'R2, and 'C' (in picofarads) are the resistor and

capacitor values of the model, respectively, and 'clk' and 'in\_data' are the clock and sinusoidal signal, respectively.

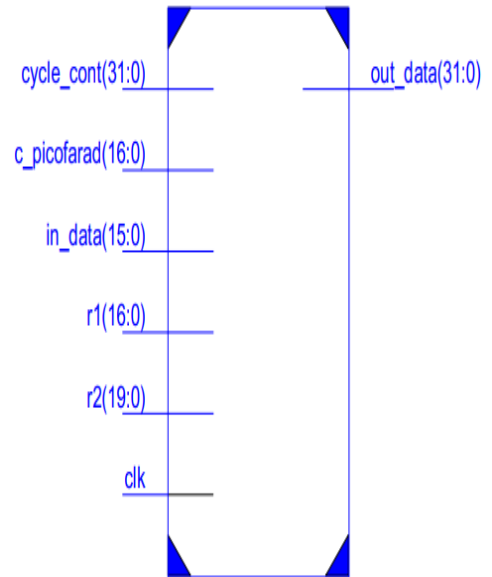


Fig. 4: General Block Diagram of the Body Model Generator in FPGA

Figure 5 shows more details of this block. As you can see, this section has 3 internal blocks, each of which will be explained later. The biofantom\_LUT block is responsible for creating LUTs, such as Tables 2 and 3, for the phase and amplitude of different body tissues at various frequencies. The cont\_delay section, as mentioned earlier, determines the number of delayed pulses given in one cycle and produces a delayed signal with a specific phase. In the z-effect section, this signal is multiplied by the value of the bioimpedance range. As a result, its output, out\_data, is both phaseshifted and amplitude-adjusted, simulating the output of the body model.

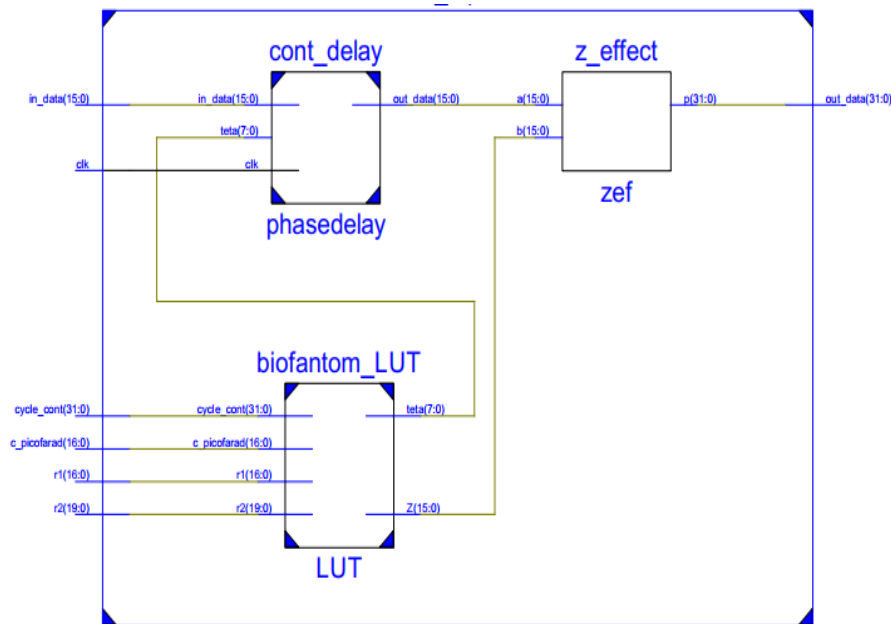


Figure 5 :Details of the Body Model Implementation Block in FPGA

**BLOCK: Z\_EFFECT**

The general form of this block is shown in Figure 6. Input a is the same shifted sine wave without amplitude change, and input b is the impedance value Z. The sinusoid from the previous step represents the current, and by multiplying it by

the impedance value, it is converted into a voltage. Therefore, the output of this block, or ' p ', is a voltage and represents the signal returned from the body phantom model.

## Implementation of human body tissues model in FPGA

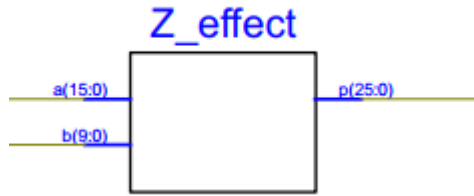


Fig 6: General Block Diagram for Creating a Shifted Sine Wave

The internal circuit of this block is a multiplier. The multiplier block is shown in Figure 7. All control inputs are active-high, and one of the multipliers can be considered a fixed number. 'A and 'B' are the inputs to the multiplier, and P is the output of the product.  $clk'$  is the system clock,  $CE$  is the clock enable, and  $SCLR'$  is used to clear the output. For this multiplier, an important aspect is that in the design wizards, one can optimize between speed and area. In this project, it has been optimized to minimize hardware size and, consequently, reduce the power consumption and the area occupied.

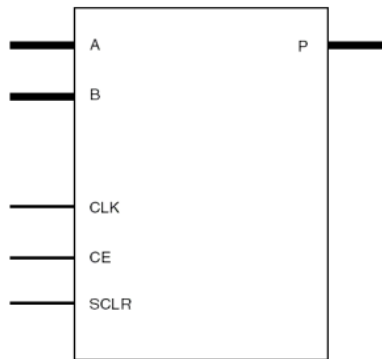


Fig. 7: Multiplier Block Diagram

The implementation of the body phantom validation program for adipose tissue is shown as an example in Figure 8. In this figure,  $R_1$ ,  $R_2$ , and  $C$  are the main input parameters of the system.  $in\_data$  is the input signal, and  $cycle\_cont$  represents the number of pulses in one cycle. The output result is visible in  $out\_data$ . The phase is generated first, and then its amplitude value is increased by the product of the input amplitude.

The phase difference value is approximately 3 degrees, which shows a slight difference from the theoretical value of 2.9981 extracted from Table 2.

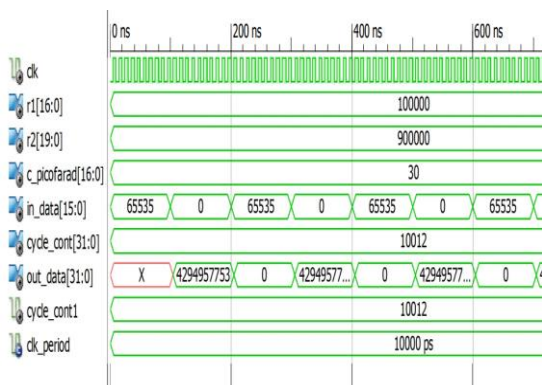


Fig. 8: Simulation Program Result of Body Phantom Validation

## Programming the program:

In the field of technology and the development of systems based on FPGA and powerful processors, using development boards like Z-Turn is one of the most common and effective methods for teaching, research, and creating innovative products. The Z-Turn board, a sophisticated combination of FPGA and ARM processors, enables engineers and scientists to rapidly convert theoretical ideas into practical prototypes with minimal cost.

After programming the critical input and output pins of the board, it is connected to a digital oscilloscope with storage capabilities through a probe. Figure 9 illustrates the connection setup.

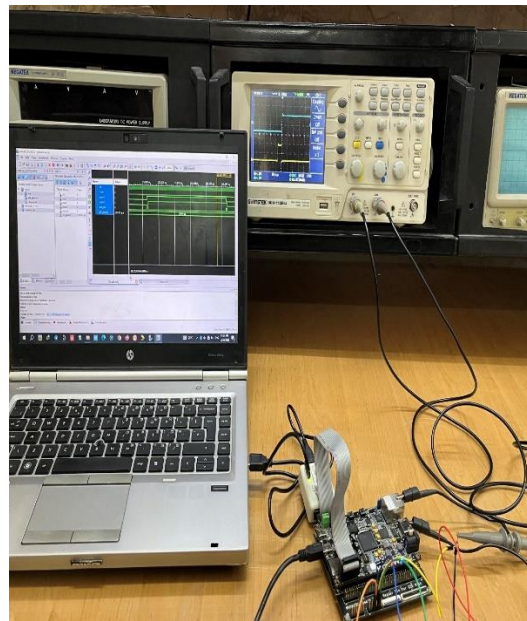


Fig. 9: Connection of the Laptop to the Programmer and Digital Oscilloscope

In the Test-Bench, which can be seen in the software output, a sinusoidal signal is converted into a square wave by passing through a comparator. This signal is delayed by a certain amount after passing through the body phantom circuit, based on the frequency values of  $R1R\_1R1$ ,  $R2R\_2R2$ , and  $CCC$ . After passing through the body model simulator, the delayed portion is determined. A 1 nanofarad capacitor is placed on each of the input and output pins to smooth the edges of the displayed signals. Oscilloscopes have the capability to store waveforms, and Figure 10 shows both the main signal and the signal passed through the model.



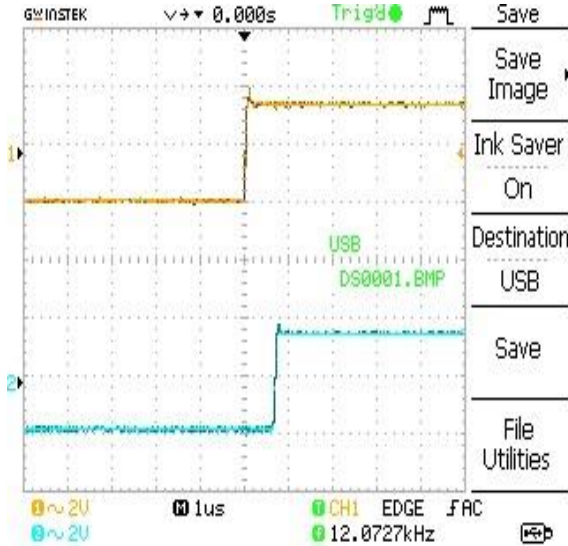


Fig. 10: Connection of the Laptop to the Programmer and Digital Oscilloscope

The example shown is for adipose tissue, which theoretically has a phase difference of 2.9981 degrees according to Table 2. The oscilloscope measurement shows a phase difference of 3 degrees, demonstrating good accuracy and precision.

### Conclusions:

As mentioned before, it is possible to implement the electrical model of body tissues on different platforms. Most research focuses on real-world implementations. Implementation on FPGA platforms has been explored in some studies, with the most comprehensive work in this field presented by Nan Li *et al.* [11]. In their research, LUTs are used to store amplitude and phase impedance information for body tissues, without performing calculations, as the numbers are directly stored.

In the current research, both the amplitude and phase of bioimpedance for 5 different body tissues at 7 frequencies are calculated within the FPGA. Based on these calculations, the tissue is simulated and implemented. A square signal was then applied to this tissue model in the FPGA, and its output was observed and recorded using a digital oscilloscope. In both simulation and real signal application cases, the difference between theoretical and practical amplitude and phase values is minimal.

### References:

- [1]. Kyle, U. G., Bosaeus, I., De Lorenzo, A., & others. (2004). Bioelectrical impedance analysis—Part II: Utilization in clinical practice. *Clinical Nutrition*, 23(6), 1145-1153.
- [2]. Meyer, C. T., Padmala, S., & Pessoa, L. (2017). Tracking dynamic threat imminence. *bioRxiv*, 183798.
- [3]. Ruiz-Vargas, A., Arkwright, J., & Ivorra, A. (2016). A portable bioimpedance measurement system based on Red Pitaya for monitoring and detecting abnormalities in the gastrointestinal tract. In *2016 IEEE EMBS Conference on Biomedical Engineering and Sciences (IECBES)* (pp. 1154-1159). IEEE.
- [4]. Vizvari, Z., Kocsis, S., & Karacsony, S. (2020). Physical validation of a residual impedance rejection method during ultra-low frequency bioimpedance spectral measurements. *Sensors*, 20(17), 4686.

- [5]. Ulbrich, M., Mühlsteff, J., Teichmann, D., Leonhardt, S., & Walter, M. (2014). A thorax simulator for complex dynamic bioimpedance measurements with textile electrodes. *IEEE Transactions on Biomedical Circuits and Systems*, 9(3), 420-412.

- [6]. Kusche, R., Malhotra, A., Ryschka, M., Ardelt, G., Klimach, P., & Kaufmann, S. (2015). A FPGA-based broadband EIT system for complex bioimpedance measurements—Design and performance estimation. *Electronics*, 4(3), -507-525.

- [7]. Luo, Y., Teng, K.-H., Li, Y., Mao, W., Heng, C.-H., & Lian, Y. (2017). A 93  $\mu$ W 11 Mbps wireless vital signs monitoring SoC with 3-lead ECG, bio-impedance, and body temperature. In *2017 IEEE Asian Solid-State Circuits Conference (A-SSCC)* (pp. 32-29). IEEE.

- [8]. Al-Hashimi, A., Nordin, A. N., & Azman, A. W. (2017). Design of a reconfigurable, modular, and multi-channel bioimpedance spectroscopy system. *Indonesian Journal of Electrical Engineering and Computer Science*, 8(2), 440-428.

- [9]. Rodriguez, S., Ollmar, S., Waqar, M., & Rusu, A. (2015). A batteryless sensor ASIC for implantable bio-impedance applications. *IEEE Transactions on Biomedical Circuits and Systems*, 10(3), 544-533.

- [10]. Simić, M., Freeborn, T. J., Šekara, T. B., Stavrakis, A. K., Jeoti, V., & Stojanović, G. M. (2023). A novel method for in-situ extracting bio-impedance model parameters optimized for embedded hardware. *Scientific Reports*, 13(1), 5070.

- [11]. Li, N., Xu, H., Zhou, Z., Xin, J., Sun, Z., & Xu, X. (2013). Reconfigurable bioimpedance emulation system for electrical impedance tomography system validation. *IEEE Transactions on Biomedical Circuits and Systems*, 7(4), -460-468. <https://doi.org/10.1109/TBCAS.2012.2224110>

- [12]. Khalil, S. F., Mohktar, M. S., & Ibrahim, F. (2014). The theory and fundamentals of bioimpedance analysis in clinical status monitoring and diagnosis of diseases. *Sensors (Basel)*, 14(6), 1010928-895. <https://doi.org/10.3390/s140610895>

### Biographies



Hossein Salarabedi was born in Neishabour, Iran, in 1972. He received the BS degree in electronics engineering from Khajeh Nasir University, Tehran, Iran, in 1995, and the MS degree in electronics engineering from Tarbiat-Modarres University, Tehran, Iran, in 1998. He has been studying for a doctorate in electronics at Azad University of

Mashhad since 2015.

## Implementation of human body tissues model in FPGA



Seyyed Javad Seyyed Mahdavi Chabok was born in Mashhad, Iran, in 1981. He received the BS degree in electrical engineering from Sharif University, Tehran, Iran, in 2002, and the MS and PhD degrees in electrical engineering from Iran University of Science and Technology, Tehran, Iran, in 2004 and 2010, respectively. In 2006, he joined the Department of Electrical and Computer Engineering at Islamic Azad University of Mashhad, where he is currently an associate professor. His research interests include modern digital circuit design, deep learning, and fault-tolerant systems design.



Mohammad Javadian Sarraf received his BSc degree in Electrical Engineering from Shahid Bahonar University in 1990. He obtained his MSc degree in Electrical Engineering from Tehran University in 1993 and his PhD degree in Electrical Engineering from University Putra Malaysia in 2013. His professional interests focus on analog integrated circuits, semiconductor and photonic devices, and sensors. Since 1996, he has been a lecturer at Islamic Azad University of Mashhad.



Hamid Reza Kobravi received the B.S. degree in electrical engineering from Ferdowsi University, Mashhad, in 2000, and the M.S. and Ph.D. degrees in biomedical engineering from Iran University of Science and Technology, Tehran, in 2004 and 2011, respectively. From 2001 to 2011, he collaborated with the Neural Technology Center at Iran University of Science and Technology, working on computer-based motor neuroprostheses for real-time movement control of paraplegic individuals. He also worked on a microcontroller-based portable neural prosthesis called PRAWALK, designed for the rehabilitation of spinal cord-injured individuals. Currently, he is an assistant professor of biomedical engineering at Azad University of Mashhad, Iran. He has supervised and co-advised more than 100 theses and research projects.